Video Article

Characterization of Electrode Materials for Lithium Ion and Sodium Ion Batteries Using Synchrotron Radiation Techniques

Marca M. Doeff[1], Guoying Chen[1], Jordi Cabana[1,2], Thomas J. Richardson[1], Apurva Mehta[3], Mona Shirpour[1], Hugues Duncan[1], Chunjoong Kim[1], Kinson C. Kam[4], Thomas Conry[5]

[1]Environmental Energy Technologies Division, Lawrence Berkeley National Laboratory

[2]Department of Chemistry, University of Illinois at Chicago

[3]Stanford Synchrotron Radiation Lightsource

[4]Haldor Topsøe A/S

[5]PolyPlus Battery Company

Correspondence to: Marca M. Doeff at mmdoeff@lbl.gov

URL: https://www.jove.com/video/50594
DOI: doi:10.3791/50594

Keywords: Physics, Issue 81, X-Ray Absorption Spectroscopy, X-Ray Diffraction, inorganic chemistry, electric batteries (applications), energy storage, Electrode materials, Li-ion battery, Na-ion battery, X-ray Absorption Spectroscopy (XAS), *in situ* X-ray diffraction (XRD)

Date Published: 11/11/2013

Citation: Doeff, M.M., Chen, G., Cabana, J., Richardson, T.J., Mehta, A., Shirpour, M., Duncan, H., Kim, C., Kam, K.C., Conry, T. Characterization of Electrode Materials for Lithium Ion and Sodium Ion Batteries Using Synchrotron Radiation Techniques. *J. Vis. Exp.* (81), e50594, doi:10.3791/50594 (2013).

Abstract

Intercalation compounds such as transition metal oxides or phosphates are the most commonly used electrode materials in Li-ion and Na-ion batteries. During insertion or removal of alkali metal ions, the redox states of transition metals in the compounds change and structural transformations such as phase transitions and/or lattice parameter increases or decreases occur. These behaviors in turn determine important characteristics of the batteries such as the potential profiles, rate capabilities, and cycle lives. The extremely bright and tunable x-rays produced by synchrotron radiation allow rapid acquisition of high-resolution data that provide information about these processes. Transformations in the bulk materials, such as phase transitions, can be directly observed using X-ray diffraction (XRD), while X-ray absorption spectroscopy (XAS) gives information about the local electronic and geometric structures (*e.g.* changes in redox states and bond lengths). *In situ* experiments carried out on operating cells are particularly useful because they allow direct correlation between the electrochemical and structural properties of the materials. These experiments are time-consuming and can be challenging to design due to the reactivity and air-sensitivity of the alkali metal anodes used in the half-cell configurations, and/or the possibility of signal interference from other cell components and hardware. For these reasons, it is appropriate to carry out *ex situ* experiments (*e.g.* on electrodes harvested from partially charged or cycled cells) in some cases. Here, we present detailed protocols for the preparation of both *ex situ* and *in situ* samples for experiments involving synchrotron radiation and demonstrate how these experiments are done.

Video Link

The video component of this article can be found at https://www.jove.com/video/50594/

Introduction

Lithium ion batteries for consumer electronics presently command an $11 billion market worldwide (http://www.marketresearch.com/David-Company-v3832/Lithium-Ion-Batteries-Outlook-Alternative-6842261/) and are the premier choice for emerging vehicular applications such as plug-in hybrid electric vehicles (PHEVs) and electric vehicles (EVs). Analogs to these devices utilizing sodium ions rather than lithium are in earlier stages of development, but are considered attractive for large scale energy storage (*i.e.* grid applications) based on cost and supply security arguments[1, 2]. Both dual intercalation systems work on the same principle; alkali metal ions shuttle between two electrodes acting as host structures, which undergo insertion processes at different potentials. The electrochemical cells themselves are relatively simple, consisting of composite positive and negative electrodes on current collectors, separated by a porous membrane saturated with an electrolytic solution usually consisting of a salt dissolved in a mixture of organic solvents (**Figure 1**). Graphite and $LiCoO_2$ are the most commonly employed negative and positive electrodes, respectively, for lithium ion batteries. Several alternative electrode materials have also been developed for specific applications, including variants of $LiMn_2O_4$ spinel, $LiFePO_4$ with the olivine structure, and NMCs ($LiNi_xMn_xCo_{1-2x}O_2$ compounds) for positives, and hard carbons, $Li_4Ti_5O_{12}$, and alloys of lithium with tin for negatives[3]. High voltage materials like $LiNi_{0.5}Mn_{1.5}O_4$, new high capacity materials such as layered-layered composites (*e.g.* $xLi_2MnO_3 \cdot (1-x)LiMn_{0.5}Ni_{0.5}O_2$), compounds with transition metals that can undergo multiple changes in redox states, and Li-Si alloy anodes are currently subjects of intense research, and, if successfully deployed, should raise practical energy densities of lithium ion cells further. Another class of materials, known as conversion electrodes, in which transition metal oxides, sulfides, or fluorides are reversibly reduced to the metallic element and a lithium salt, are also under consideration for use as battery electrodes (primarily as replacements for anodes)[4]. For devices based on sodium, hard carbons, alloys, NASICON structures, and titanates are being investigated for use as anodes and various transition metal oxides and polyanionic compounds as cathodes.

Because lithium ion and sodium ion batteries are not based on fixed chemistries, their performance characteristics vary considerably depending on the electrodes that are employed. The redox behavior of the electrodes determines the potential profiles, rate capabilities, and cycle lives of the devices. Conventional powder X-ray diffraction (XRD) techniques can be used for initial structural characterization of pristine materials and *ex situ* measurements on cycled electrodes, but practical considerations such as low signal strength and the relatively long times needed to collect data limit the amount of information that can be obtained on the discharge and charge processes. In contrast, the high brilliance and short wavelengths of synchrotron radiation (*e.g.* λ=0.97 Å at the Stanford Synchrotron Radiation Lightsource's beamline 11-3), combined with the use of high throughput image detectors, permit acquisition of high-resolution data on samples in as little as 10 sec. *In situ* work is performed in transmission mode on cell components undergoing charge and discharge in hermetically sealed pouches transparent to X-rays, without having to stop operation to acquire data. As a result, electrode structural changes can be observed as "snapshots in time" as the cell cycles, and much more information can be obtained than with conventional techniques.

X-ray absorption spectroscopy (XAS), also sometimes referred to as X-ray Absorption Fine Structure (XAFS) gives information about the local electronic and geometric structure of materials. In XAS experiments, the photon energy is tuned to the characteristic absorption edges of the specific elements under investigation. Most commonly for battery materials, these energies correspond to the K-edges (1s orbitals) of the transition metals of interest, but soft XAS experiments tuned to O, F, C, B, N and the $L_{2,3}$ edges of first row transition metals are also sometimes carried out on *ex situ* samples[5]. The spectra generated by XAS experiments can be divided into several distinct regions, containing different information (see Newville, M., Fundamentals of XAFS, http://xafs.org/Tutorials?action=AttachFile&do=get&target=Newville_xas_fundamentals.pdf). The main feature, consisting of the absorption edge and extending about 30-50 eV beyond is the X-ray Absorption Near Edge Structure (XANES) region and indicates the ionization threshold to continuum states. This contains information about the oxidation state and coordination chemistry of the absorber. The higher energy portion of the spectrum is known as the Extended X-ray Absorption Fine Structure (EXAFS) region and corresponds to the scattering of the ejected photoelectron off neighboring atoms. Fourier analysis of this region gives short-range structural information such as bond lengths and the numbers and types of neighboring ions. Preedge features below the characteristic absorption energies of some compounds also sometimes appear. These arise from dipole forbidden electronic transitions to empty bound states for octahedral geometries, or dipole allowed orbital hybridization effects in tetrahedral ones and can often be correlated to the local symmetry of the absorbing ion (*e.g.* whether it is tetrahedrally or octahedrally coordinated)[6].

XAS is a particularly useful technique for studying mixed metal systems such as NMCs to determine initial redox states and which transition metal ions undergo redox during delithiation and lithiation processes. Data on several different metals can be obtained rapidly in a single experiment and interpretation is reasonably straightforward. In contrast, Mossbauer spectroscopy is limited to only a few metals used in battery materials (primarily, Fe and Sn). While magnetic measurements can also be used to determine oxidation states, magnetic coupling effects can complicate interpretation particularly for complex oxides such as the NMCs.

Well-planned and -executed *in situ* and *ex situ* synchrotron XRD and XAS experiments give complementary information and allow a more complete picture to be formed of the structural changes occurring in electrode materials during normal battery operation than what can be obtained via conventional techniques. This, in turn, gives a greater understanding of what governs the electrochemical behavior of the devices.

Protocol

1. Planning of Experiments

1. Identify beam line experiments of interest. Refer to beam line webpages as guides. For SSRL XAS and XRD, these are: http://www-ssrl.slac.stanford.edu/beamlines/bl4-1/ and http://www-ssrl.slac.stanford.edu/beamlines/bl4-3/ and http://www-ssrl.slac.stanford.edu/beamlines/bl11-3/
    1. Contact beam line scientist and discuss details of experiment.
2. Check deadlines and requirements for proposals by going to the relevant website.
3. Write beam time proposal and submit.
4. After the proposal has been scored, schedule beam time.
5. Follow instructions provided by the facility to prepare for beam time. Consider the details of the experiment, transport of materials (especially of devices containing alkali metals) and equipment, and any safety concerns. Safety training is generally required for new users.

2. Preparation of Materials, Electrodes, and Cells

1. Synthesize or obtain active material of interest.
2. Characterize material by conventional X-ray powder diffraction, using steps 2.2.1-2.2.9.
    1. Grind powder and sieve to ensure uniform particle size distribution.
    2. Load sample into sample holder. Remove backplate from holder and place it against a glass slide. Fill cavity with powder, then attach backplate, flip holder and remove slide. This ensures that the powder is even with the surface of the holder and that the surface is flat.
    3. Log into logbook for the diffractometer.
    4. Insert sample holder into diffractometer and align.
    5. Close doors of diffractometer.
    6. Using Data Collector program on computer attached to Panalytical diffractometer, increase voltage and current to values appropriate for measurement. Select slits and beam masks for the experiment. Select or modify program for scan.
    7. Start program and name datafile. Lock diffractometer doors by swiping badge when prompted by the program. Collect data.
    8. Analyze pattern using High Score program. In particular, look for the presence of impurities (extra reflections) and whether pattern matches that of reference materials or calculated patterns.
    9. Remove sample from diffractometer. Turn down current and voltage, and close doors. Log out, noting any unusual conditions.

3. Obtain scanning electron micrographs to assess particle morphologies, using steps 2.3.1-2.3.10.
    1. Prepare sample by attaching carbon tape to an aluminum stub, and sprinkling sample powder onto sticky side. Test for magnetism by holding a kitchen magnet over the sample.
    2. Insert sample into SEM chamber via airlock.
    3. Once vacuum is established, turn accelerating voltage on.
    4. In low magnification mode, adjust contrast and brightness. This is most conveniently done using the ACB button.
    5. Find area of interest by manually scanning in the x and y directions.
    6. Switch to SEM or gentle beam modes if higher magnification is desired. Select desired detector, and set working distance to values appropriate for the experiment.
    7. Adjust contrast and brightness using ACB knob.
    8. Focus image with stage z control.
    9. Align beam, correct astigmatism and focus using x and y knobs.
    10. Take pictures as desired, using photo button, and save to appropriate folder on the computer.
    11. When finished, turn off accelerating voltage. Move sample to exchange position and remove from chamber via airlock.

4. Conduct elemental analysis by ICP if needed, and characterize materials with any other desired techniques such as IR or Raman spectroscopy.
5. Fabricate electrodes, using steps 2.5.1-2.5.8.
    1. Make a solution of 5-6% (wt.) polyvinylidene fluoride (PVDF) in N-methylpyrolidinone (NMP).
    2. Mill together active material and conductive additive (acetylene black, graphite, *etc.*).
    3. Add NMP solution from step 2.3.1 to dry powder from step 2.3.2 and mix. Proportions vary depending on the nature of the active material, but a final dry composition of 80:10:10 (active material:PVDF:conductive additive) is common.
    4. Using a doctor blade and (optionally) a vacuum table, cast electrode slurry onto an Al or Cu current collector. Carbon coated Al foil may be used for Li-ion battery cathode materials and all Na-ion electrode materials, and Cu foil is used for Li-ion anode materials.
    5. Allow electrodes to air-dry.
    6. Dry electrodes further using an IR lamp, hot plate, or vacuum oven.
    7. Cut or punch electrodes to the size needed. Weigh electrodes.
    8. Transfer electrodes to an inert atmosphere glovebox. An additional drying step using a vacuum heated antechamber attached to the glovebox is recommended to remove all residual moisture.

6. Assemble electrochemical devices (usually coin cells, but other configurations can be used for electrochemical characterization) for initial characterization, *ex situ* samples, and/or beam line experiment, using steps 2.6.1-2.6.7.
    1. Gather all needed components in the inert atmosphere glovebox.
    2. Cut lithium or sodium foil to the desired size.
    3. Cut microporous separator to the desired size.
    4. Layer components in this order in the device: electrode, separator, electrolytic solution, and Li or Na foil.
    5. Add spacers and wave washers as needed.
    6. Seal cell using a coin cell press.
    7. For *in situ* XRD experiments, attach tabs to either side of coin cell and seal device in polyester pouch.

7. Perform electrochemical experiment for initial characterization or *ex situ* work, using steps 2.7.1-2.7.6.
    1. Connect leads from the potentiostat/galvanostat or cycler to device and measure open circuit potential.
    2. Write program for the electrochemical experiment desired or select an archived program.
    3. Run experiment and collect data.
    4. For *ex situ* experiments, disassemble the device in glovebox, taking care not to short-circuit it. For coin cells, use either a coin cell disassembler tool or pliers wrapped with Teflon tape.
    5. Rinse electrodes with dimethylcarbonate to remove residual electrolyte salt. Allow them to dry.
    6. Cover electrodes for *ex situ* study with Kapton foil for XRD experiments or scotch tape for XAS and store in the glovebox until the experiment is carried out.

8. Powders intended for study by XAS should be sieved to ensure particle size homogeneity. They may then be sprinkled onto several pieces of scotch tape. A series of samples can then be prepared by stacking progressively more numerous pieces of the powdered tape together. This is particularly useful if the user is uncertain about the amount of powder needed for the optimal signal.
    1. Alternatively, powders for XAS measurements may be diluted with BN if the user is confident about what will result in the optimum signal.

3. Performance of Experiments at the Synchrotron Facility

1. Several days before the experiment is to begin, plan transport of materials and equipment to the facility.
    1. For devices containing alkali metal anodes, shipping is required to avoid hazards associated with transportation in personal or public vehicles.
    2. Equipment such as portable galvanostat/potentiostats and laptop computers and nonhazardous samples such as electrodes for *ex situ* work may be brought to the facility by the individual carrying out the experiments in any convenient fashion.

2. Check in and register at the facility.
3. For both *in situ* and *ex situ* XRD experiments, take a reference pattern of LaB_6 for purposes of calibration.
    1. Contact beamline scientist and personnel for instructions.
    2. Calibrate beam to find right beam conditions.

3. Measure reference pattern of LaB_6.

4. For *in situ* XRD experiments, set up device and start experiment following steps 3.4.1-3.4.6.
    1. Insert pouch into Al pressure plates and ensure that holes are properly aligned to allow the X-ray beam to transmit.
    2. Find optimum beam position and exposure time. Prolonged exposure can lead to oversaturation. Decide whether sample will be rocked or stationary.
    3. Take initial pattern before electrochemistry is started.
    4. Attach leads from galvanostat/potentiostat to device.
    5. Start electrochemistry experiment.
    6. Obtain data. Once experiment is under way, data collection is automatic, and user need only to oversee to make sure experiment is going as planned.

5. Set up XAS experiments.
    1. Check in and contact beamline scientist and personnel for instructions.
    2. Insert sample and foil reference material (depending on metal that is being measured; *e.g.* Ni for Ni K edge).
    3. Align sample.
    4. Determine energy of specific metal edge using IFEFFIT's Hephaestus. Tune monochromator, then de-tune by about 30 % to eliminate higher order harmonics. Change gains to adjust I_1 and I_2 measure offsets.
    5. Take measurement. Two or more scans should be taken and merged for the element of interest.
    6. Repeat steps 3.5.3 to 3.5.5 for additional elements, as needed.

4. Data Analysis

1. For XRD work, calibrate the LaB_6 image.
    1. Download Area Diffraction Machine, which is available through the Google code (http://code.google.com/p/areadiffractionmachine/).
    2. Open the image for LaB_6 diffraction and use initial calibration values from the file header.
    3. Open the reference Q (=2π/d) values of LaB_6.
    4. Calibrate the LaB_6 diffraction image with the Q values and the initial guess of the calibration values**.**
    5. Obtain correct calibration values by image fitting.
    6. Save the calibration values into the calibration file.

2. Calibrate the data images from the experiment.
    1. Open the diffraction images from the experiment.
    2. Open the calibration file from the LaB_6 reference (saved in step 4.1.6).
    3. Open the reference Q (=2π/d) values of Al or Cu (current collectors for the electrodes) and use them as internal references.
    4. Calibrate the pattern images by image fitting.
    5. Integrate the image to Q vs. Intensity data (line scans).
    6. Fit patterns using the desired fitting program (CelRef, Powdercell, RIQAS, GSAS, *etc.*).

3. Process electrochemical data using any convenient plotting program (Excel, Origin, KaleidaGraph, Igor, *etc.*).
4. For XAS data, use ARTEMIS/ATHENA in the IFEFFIT software package for analysis.
    1. Calibrate data using the first peak in the derivative of the absorption spectra of the reference metals.
    2. Merge like scans.
    3. Subtract background and normalize data.
    4. Use the AUTOBK function to isolate the EXAFS data.
    5. Fourier transform the EXAFS data.
    6. Use a least squares fit to the Fourier transformed spectra in R or k space to extract structural information.

Representative Results

Figure 2 shows a typical sequence used for an *in situ* experiment. After synthesis and characterization of active material powders, composite electrodes are prepared from slurries containing the active material, a binder such as polyvinylidene fluoride (PVDF) and conductive additives such as carbon black or graphite suspended in N-methylpyrrolidinone (NMP), cast onto either aluminum or copper foil current collectors. Aluminum is used for lithium ion battery cathodes and all sodium ion battery electrodes, and copper is used for lithium ion battery anodes. After the electrodes are dried, cut, and weighed, cells are assembled in an inert atmosphere glovebox using microporous separators, the appropriate electrolytic solutions and negative electrodes consisting of either Li or Na foils. These components are then hermetically sealed in a protective pouch, made of polyester, which keeps out air and is reasonably X-ray transparent. Aluminum and nickel tabs are used to make electrical contacts to the positive and negative electrodes, respectively. The Al tabs are ultrasonically welded to the cathode current collectors, while the soft Li or Na metal used as the anode is simply pressed around the Ni tab to make contact. To maintain pressure, the pouch cell is compressed between two metal plates with 2 mm holes cut into them to allow the transmission of X-rays. Poor contact between cell components may result in high overpotentials and premature cutoff, particularly if voltage limits are not adjusted to accommodate the additional overpotential encountered in this configuration. Excessive pressure, on the other hand, may cause cell shorting and failure of the experiment. Better pressure control is achieved when components are first assembled into a coin cell with small holes drilled into the casings and spacers, which is then sealed into the protective pouch after tabs are attached. Wave washers and spacers are used to fill any extra volume in the device, maintain pressure, and ensure good contact among the components.

A small portable potentiostat/galvanostat and laptop computer are then used to perform the electrochemical experiment and collect data at the beam line. One charge-discharge cycle typically takes about 20 hr to complete. The cycle is usually performed galvanostatically (*i.e.* using constant current) between preselected voltage limits. The sample may either be kept stationary, rocked (left/right or up/down) or rotated around the beam axis in the beam line. Advantages to the last two are that results are obtained over a somewhat larger area of the electrode, effects of preferred orientation in powder-containing electrodes are minimized, and counting statistics are improved.

Transmission XRD ring patterns (see **Figure 2**, step 5) can be obtained in about 10 sec, with a data readout time of about 1-2 min. Integration of calibrated image patterns yields line scans (intensity vs. Q). Beam line 11-3 at the Stanford Synchrotron Radiation Lightsource uses a single Si(311) monochromator, generating an incident wavelength of approximately 0.97 Å (12,735 eV), though energy fluctuations on the order of a few eVs (~0.01%) due primarily to diurnal cycling (daily temperature fluctuations) are often observed over the course of the lengthy charge and discharge measurements. Thus, image calibration for each scan is essential to de-convolute the diffraction pattern changes. Calibration is performed with The Area Diffraction Machine software developed in conjunction with the 11-3 beam line (http://code.google.com/p/areadiffractionmachine/).

Figure 3 shows *in situ* XRD data obtained on a Li/$Li_x[Ni_{0.45}Mn_{0.45}Co_{0.05}Al_{0.05}]O_2$ cell which underwent charge (in black) and discharge (in green), after calibration and conversion of the ring patterns to line scans. Peaks arising from cell components including the Al current collector, polyester pouch, and polypropylene separator are marked with red and blue dots (lithium metal is essentially transparent to X-rays, but additional peaks will arise if sodium metal anodes are used). Indexed reflections attributable to the $Li_x[Ni_{0.45}Mn_{0.45}Co_{0.05}Al_{0.05}]O_2$ active material are marked on the patterns. Because the unit cell parameters changed as a function of x (Li content), peaks due to this phase and the Al current collector overlapped in some of the patterns. The interference from cell components presented significant challenges both for perfect background subtraction and Rietveld refinement of the entire diffraction patterns. To circumvent this problem, backgrounds were manually subtracted, and a limited set of peaks that did not overlap with cell components were selected for the fitting. Unit cell parameters at various states-of-charge were subsequently calculated by a least-squares refinement using the available peak positions and the program CelRef (http://www.ccp14.ac.uk/tutorial/lmgp/celref.htm). The degree to which cell components interfere in patterns obtained from *in situ* experiments vary depending on the nature of the material under study, and these problems are not always encountered. In that case, any convenient refinement or fitting program may be used to analyze data (GSAS, PowderCell, RIQAS, FullProf, *etc*.).

Due to time constraints, it is sometimes preferable to perform synchrotron XRD experiments *ex situ*. It is obviously not practical to perform multiple cycles over a long time in the beam line, for example. Instead, electrodes can be removed from cycled cells, rinsed with solvent to remove residual electrolyte salt, dried, and covered with Kapton film to provide protection from air, for later examination. Additionally, it can be useful to study a few electrodes at different states-of-charge harvested from electrochemical cells, to give an idea of what to expect from a more involved *in situ* experiment performed later. These experiments are much simpler to carry out and much less time-consuming; several samples can usually be run in an hour. An additional benefit to the *ex situ* work is the absence of most interfering cell components, although signals from the current collector, binder and conductive additives are usually still observed and the Kapton itself contributes to the background. Caveats for *ex situ* work are that washing and long or improper storage may change or degrade the sample. In worst-case scenarios, the data obtained *ex situ* may not even provide relevant information because of these problems. If appropriate caution is maintained, however, *ex situ* work can still be of some value, although direct observation of processes using *in situ* configurations is clearly the most desirable option whenever time constraints allow.

Because XAS experiments are element-specific, interference from cell components other than the electrode material of interest are not as problematic as with XRD (assuming that cell hardware does not contain the metals of interest). Only one absorption edge (element) can be measured at a time, however. While switching to a new energy takes only seconds, tuning, changing gains and offsets on the ion chambers, changing reference foils, and purging with gas may take up to an additional ten minutes. Switching from one element to another during an *in situ* run may result in some loss of data. Meaningful EXAFS data can be difficult to obtain during *in situ* work, because the structural changes that are occurring often have similar time constants to that of the measurements themselves. Another consideration is that XAS beam lines are often heavily subscribed, meaning limited time for each user. For these reasons, it is generally more practical to carry out XAS experiments on *ex situ* samples rather than perform *in situ* work (although see reference 7 for an example of *in situ* work). Obtaining data on *ex situ* samples can take anywhere from a few minutes to one hour depending on how many elements are being studied and the facility at which the work is carried out. During each edge measurement, a similar metal foil (*e.g.* Ni, Mn, or Co) spectrum should be recorded for energy reference. This is carried out simultaneously with the sample measurement. In addition, the user may wish to record data on reference materials containing the metals of interest with known oxidation states, separately, particularly if unusual redox states are involved in the electrochemistry. For example, Li_3MnO_4 was used as a reference for a recent study of a series of lithium manganese oxynitride electrode materials to verify the presence of tetrahedrally coordinated Mn^{5+}.[8]

Most XAS experiments directed towards studying bulk processes in electrode materials are run in transmission mode, which is suitable when molar concentrations of the elements of interest are above about 5-10% (http://xafstraining.ps.bnl.gov). Best results are obtained when the thickness of the sample, x, is adjusted so that $\mu x<3$ above the absorption edge. If the absorption coefficient (μ) is not known (*e.g.* for complex materials, which includes many battery electrode materials), it can be useful to start with a very small amount of powder sprinkled onto the sticky side of a piece of scotch tape. One or more additional pieces of powdered scotch tape can be attached to the original to increase the signal to the point where the optimum response is obtained (typically, corresponding to one absorption length). For materials where the absorption coefficient is known, the sample can be diluted with BN so that the correct absorption is obtained at a given thickness.

At SSRL, Ni, Mn, and Co K-edges can be studied at beam line 4.1, while Ti and S edges are investigated at beam line 4.3. Detuning the double crystal monochromator by about 30% eliminates higher order harmonics. Calibration is carried out using the first peak in the derivative of the absorption spectra of the reference metals. Duplicate scans can be run and merged after alignment to improve the quality of the data. Artemis/Athena from the software package IFEFFIT are used for analysis[9]. After merging like-scans, the background contribution is subtracted and the data is normalized. EXAFS data is isolated using the AUTOBK function, and is Fourier transformed. Least squares fitting to the Fourier transformed spectrum in R or k space is then used to extract structural information. An example of XAS data, taken at the Mn K edge, is shown in **Figure 2**, step 5 and the XANES and EXAFS regions are marked on the spectrum.

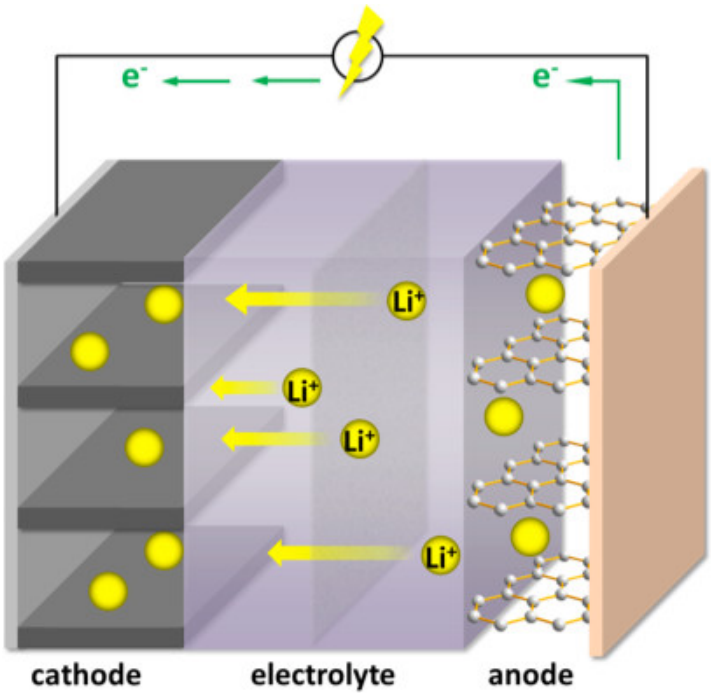

Figure 1. Schematic of a Li-ion battery with a graphite anode and layered metal oxide cathode undergoing discharge. Used with permission from reference 3.

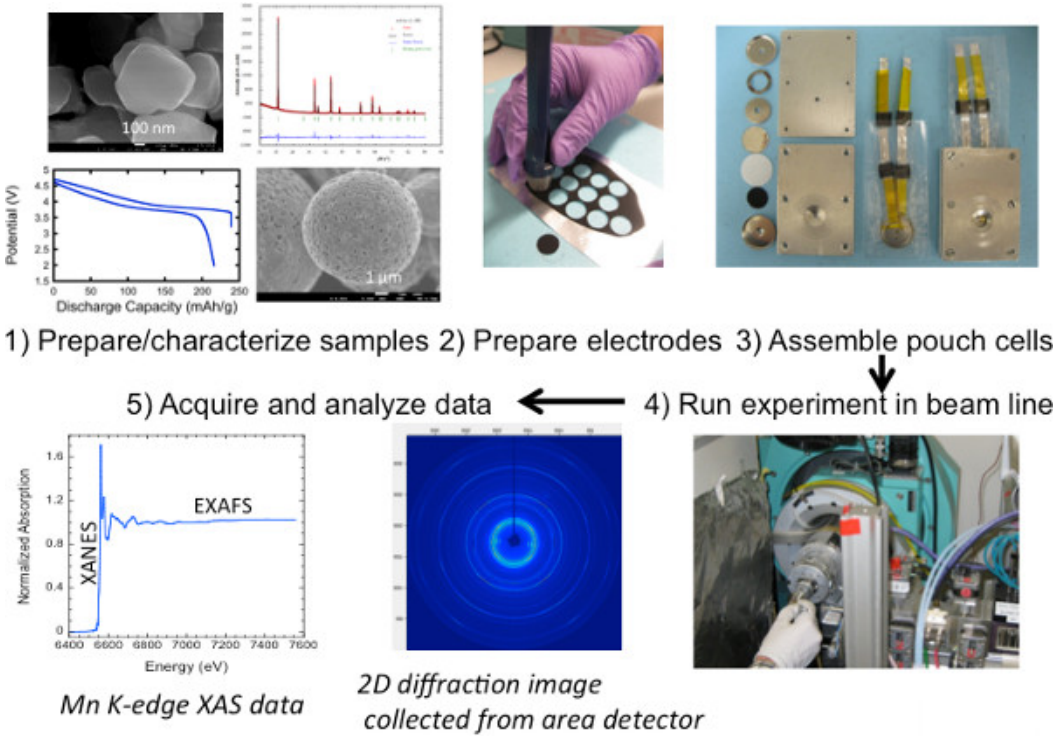

Figure 2. Typical sequence of an *in situ* experiment. Steps include 1) preparation and characterization of the sample, 2) preparation of composite electrodes, 3) assembly of pouch cells, 4) set up of an *in situ* experiment in the beamline, and 5) data acquisition and analysis.

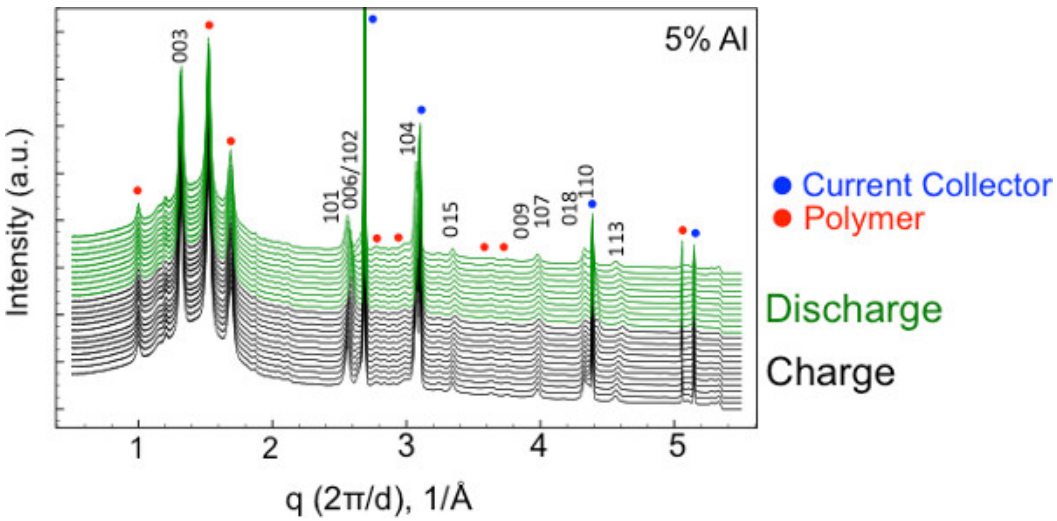

Figure 3. Line scans obtained by integrating image scans on a Li/Li$_x$[Ni$_{0.45}$Mn$_{0.45}$Co$_{0.05}$Al$_{0.05}$]O$_2$ cell undergoing charge (black) and discharge (green). Reflections attributed to the Al current collector and polymeric cell components (pouch and microporous separator) are marked with blue and red dots, respectively.

Table 1. Table of Materials.

Table 2. Table of Equipment.

Discussion

Analysis of XANES data indicates that as-made $LiNi_xCo_{1-2x}Mn_xO_2$ ($0.01 \le x \le 1$) compounds contains Ni^{2+}, Co^{3+}, and Mn^{4+}.[10] A recent *in situ* XAS study on $LiNi_{0.4}Co_{0.15}Al_{0.05}Mn_{0.4}O_2$ showed that Ni^{2+} was oxidized to Ni^{3+} and, ultimately, Ni^{4+} during delithiation, but that redox processes involving Co^{3+} contributed some capacity even at low states-of-charge, contrary to previous assumptions[7]. Another study involving the low cobalt compositions, $LiNi_{0.45}Co_{0.1-y}Al_yMn_{0.45}O_2$, also indicated that Co was electroactive at the early stages of delithiation[11].

Synchrotron XRD[12] and XAS[11] studies of a series of NMCs with the composition $LiNi_{0.45}Mn_{0.45}Co_{0.1-y}Al_yO_2$ ($0 \le y \le 0.1$) have yielded insights into the improved electrochemical performance of the Al-substituted variants. Analysis of high-resolution synchrotron XRD patterns obtained on the pristine powders indicated that the y=0.1 material exhibits a slight monoclinic distortion, not discernible in the conventional powder XRD patterns. To relieve strain in the transition metal planes, which consist of metal-containing edge-shared octahedra with different equilibrium M-O distances, local scale ordering occurs, resulting in the distortion. The strain-relieving distortion was further confirmed by close examination of the EXAFS data[11]. Electrochemical cycling induces additional strain, though the observed changes in the EXAFS data were smaller for electrodes containing Al. *In situ* XRD experiments on Li cells containing these NMC cathodes indicated that lattice changes during cell charge (delithiation) were smaller for the Al-substituted materials than for the unsubstituted baseline. Fewer structural changes upon prolonged cycling were also observed in the Al-containing electrodes.

Partial Al-substitution has also been proposed as a possible means to stabilize orthorhombic $LiMnO_2$ electrodes[13]. This material rapidly converts from the original zigzag layered structure to spinel upon electrochemical cycling, with a concomitant deterioration of the electrochemical properties. However, no stabilization effect was observed during *in situ* XRD experiments on an electrode substituted with 25% Al; in fact, reflections attributable to spinel formation were observed even during the initial cell charge[14].

The degree of transition metal ordering in the high voltage spinel with the nominal composition $LiNi_{0.5}Mn_{1.5}O_4$ is expected to affect the voltage profile and other electrochemical characteristics of the material in operating cells[15]. In ordered materials (space group $P4_332$), the Ni and Mn occupy *4a* and *12d* octahedral sites, respectively, whereas in the disordered variants (space group Fd3_m) the transition metals are distributed randomly over octahedral *16d* sites. A comparison of synchrotron xrd patterns obtained on two samples with differing degrees of transition metal ordering in an *in situ* experiment revealed very different phase behavior during delithiation processes[16]. The disordered material exhibited a wide solid solution region during the initial delithiation, with two narrow two-phase regions observed at high states-of-charge. The solid solution region was much smaller for the ordered material, and the coexistence of three phases was observed at a composition of about x=0.3 in $Li_xNi_{0.5}Mn_{1.5}O_4$, flanked by two small two-phase regions. The dissimilarities in the phase behaviors, which are thought to be due to variations in lithium-vacancy ordering schemes, have been proposed as an explanation for rate capability differences observed between ordered and disordered $LiNi_{0.5}Mn_{1.5}O_4$. Contrary to expectations, however, the more ordered material in reference 16 performed better in this regard than the disordered sample. This was attributed to morphology effects; particles of the disordered sample consisted of plates with exposed (112) facets, whereas those of the ordered material were octahedral with (111) surface facets.

In addition to ordering and morphology effects, the physical and electrochemical characteristics of $LiNi_{0.5}Mn_{1.5}O_4$ are also dependent on impurity content and the amount of Mn^{3+} present. During the high temperature processing used during synthesis, a Ni-containing rock salt impurity is formed and some Mn^{4+} is reduced to Mn^{3+} in the main phase. It can be difficult to detect small amounts of the rock salt impurity because of peak overlap in the XRD patterns, or to determine its exact composition, which varies with the thermal treatment. Analysis of Ni and Mn K edge XANES data revealed the presence of a significant amount of rock salt impurity containing both Ni and Mn in a sample made at 1,000 °C[17].

The techniques described here were directed towards understanding bulk processes in electrodes undergoing charge and discharge. The assumption is that the structural changes observed using the very small spot size (*e.g.* 0.15 mm x 0.15 mm at beam line 11-3) for the experiment are typical of the electrode as a whole. This is generally true for well-made electrodes and cells, using the low current densities and relatively long charge-discharge times described above. *Ex situ* results have also generally been obtained on electrodes in cells subjected to normal operation, which have then undergone equilibration. In some circumstances, however, it can be instructive to obtain results under nonequilibrium conditions to gain understanding of failure modes of battery electrodes during operation at high current densities or under various abuse conditions. Nonuniform charge distributions may occur in these situations, particularly if electrodes or cells are unoptimized. The nonuniformity may result in local areas of overcharge or discharge, causing structural degradation that ultimately results in reduced performance and safety of the device. A synchrotron X-ray microdiffraction technique has recently been used to map charge distribution in $LiFePO_4$ electrodes charged at high rates[18]. Although this was performed *ex situ*, the two-phase nature of the $LiFePO_4$ redox reaction essentially prevented relaxation of the charge distribution once the current was interrupted. For this experiment, partially charged electrodes were step-scanned using a monochromatic (6.02 keV) X-ray beam and a diffraction pattern was collected for each step. Scanning was carried out both perpendicular and parallel to the current collector on electrodes taken from partially charged coin cells and prismatic cells. In both cases, unequal distribution of charge was observed, with the surface of coin cell electrodes more highly charged than the active material close to the current collector, and the portion closest to the tab the most highly charged for the electrode taken from the prismatic cell.

These results illustrate the importance of good spatial as well as temporal resolution in synchrotron experiments directed towards a full understanding of battery operation. As the field advances, new techniques geared to imaging electrode materials in 3D are being developed. One such example is the combined use of full-field X-ray microscopy (TXM) with XANES to follow chemical and morphological changes in NiO electrodes as they underwent conversion to Ni and Li_2O during cell discharge[19]. A particular challenge for these experiments, however, can be handling the large amount of data that is generated.

New high throughput inelastic X-ray scattering configurations have also been used recently to obtain finer detail on the functioning of battery materials. Examples include a combined soft XAS (Fe L-edge) and hard X-ray Raman scattering study of $LiFePO_4$ electrodes, done *ex situ*[20]. The latter combines the advantages of a hard X-ray technique (*e.g.* ability to probe bulk phenomena and, eventually, to perform experiments *in situ* under a variety of conditions) with the sensitivity associated with soft X-ray XAS, and can be used for low z elements such as carbon and oxygen[21]. Nonresonant inelastic X-ray scattering (NIXS) has also been used to measure the lithium and oxygen K-edges of Li_2O_2 (the discharge product of lithium/air batteries with organic electrolytes), resulting in a better understanding of its structure[22]. The sensitivity of NIXS lends it particularly well for situations where poorly crystalline materials are encountered (such as in batteries undergoing discharge).

Disclosures

Authors have nothing to disclose.

Acknowledgements

This work is supported by the Assistant Secretary for Energy Efficiency and Renewable Energy, Office of Vehicle Technologies of the U.S. Department of Energy under Contract No. DE-AC02-05CH11231. Portions of this research were carried out at the Stanford Synchrotron Radiation Lightsource, a Directorate of SLAC National Accelerator Laboratory and an Office of Science User Facility operated for the U.S. Department of Energy Office of Science by Stanford University. The SSRL Structural Molecular Biology Program is supported by the DOE Office of Biological and Environmental Research, and by the National Institutes of Health, National Center for Research Resources, Biomedical Technology Program (P41RR001209).

References

1. Kim, S.-W., Seo, D.-I., Ma, X., Ceder G., & Kang, K. Electrode Materials for Rechargeable Sodium-Ion Batteries: Potential Alternatives to Current Lithium-Ion Batteries. *Adv. Energy Mater.* **2**, 710-721 (2012).
2. Palomares, V., Serras, P., Villaluenga, I., Huesa, K.B., Cerretero-Gonzalez, J., & Rojo, T. Na-ion Batteries, Recent Advances and Present Challenges to Become Low Cost Energy Storage Systems. *Energy Environ. Sci.* **5**, 5884-5901 (2012).
3. Kam, K.C., & Doeff, M.M. Electrode Materials for Lithium Ion Batteries. *Materials Matters*. **7,** 56-60 (2012).
4. Cabana, J., Monconduit, L., Larcher, D., & Palacin, M.R. Beyond Intercalation-Based Li-Ion Batteries: The State of the Art and Challenges of Electrode Materials Reacting Through Conversion Reactions. *Adv. Energy Mater.* **22**, E170-E192 (2010).
5. McBreen, J. The Application of Synchrotron Techniques to the Study of Lithium Ion Batteries. *J. Solid State Electrochem.* **13**, 1051-1061 (2009).
6. de Groot, F., Vankó, G., & Glatzel, P. The 1s X-ray Absorption Pre-edge Structures in Transition Metal Oxides. *J. Phys. Condens. Matter.* **21**, 104207 (2009).
7. Rumble, C., Conry, T.E., Doeff, M., Cairns, E.J., Penner-Hahn, J.E., & Deb, A. , Structural and Electrochemical Investigation of $Li(Ni_{0.4}Co_{0.15}Al_{0.05}Mn_{0.4})O_2$. *J. Electrochem. Soc.* **157**, A1317-A1322 (2010).
8. Cabana, J., Dupré, N., Gillot, F., Chadwick, A.V., Grey, C.P., & Palacín, M.R. Synthesis, Short-Range Structure and Electrochemical Properties of New Phases in the Li-Mn-N-O System. *Inorg. Chem.* **48**, 5141-5153 (2009).
9. Ravel, B., & Newville, M. ATHENA, ARTEMIS, HEPHAESTUS: data analysis for X-ray absorption spectroscopy using IFEFFIT. *Journal of Synchrotron Radiation.* **12,** 537-541 (2005).
10. Zeng D., Cabana, J. Bréger, Yoon, W.-S., & Grey, C.P. Cation Ordering in $Li[Ni_xMn_xCo_{(1-2x)}]O_2$-Layered Cathode Materials: A Nuclear Magnetic Resonance (NMR), Pair Distribution Function, X-ray Absorption Spectroscopy, and Electrochemical Study. *Chem. Mater.* **19,** 6277-6289 (2007).
11. Conry, T.E., Mehta, A., Cabana, J., & Doeff, M.M. XAFS Investigation of $LiNi_{0.45}Mn_{0.45}Co_{0.1-y}Al_yO_2$ Positive Electrode Materials. *J. Electrochem. Soc.* **159**, A1562-A1571(2012).

12. Conry, T.E., Mehta, A., Cabana, J., & Doeff, M.M. Structural Underpinnings of the Enhanced Cycling Stability upon Al-substitution in $LiNi_{0.45}Mn_{0.45}Co_{0.1-y}Al_yO_2$ Positive Electrode Materials for Li-ion Batteries. *Chem. Mater.* **24,** 3307-3317 (2012).
13. Reed, J., & Ceder, G. Role of Electronic Structure in the Susceptibility of Metastable Transition-Metal Oxide Structures to Transformation. *Chem. Rev.* **104**, 4513-4534 (2004).
14. Cook, J.B., Kim, C., Xu, L., & Cabana, J. The Effect of Al Substitution on the Chemical and Electrochemical Phase Stability of Orthorhombic $LiMnO_2$. *J. Electrochem. Soc.* **160**, A46-A52 (2013).
15. Lee, E., & Persson, K. Revealing the Coupled Cation Interactions Behind the Electrochemical Profile of $LixNi_{0.5}Mn_{1.5}O_4$. *Energy Environ. Sci.* **5**, 6047-6051 (2012).
16. Hai, B., Shukla, A.K., Duncan, H., & Chen, G. The Effect of Particle Surface Facets on the Kinetic Properties of $LiMn1.5Ni_{0.5}O_4$ Cathode Materials. *J. Mater. Chem. A.* **1**, 759-769 (2013).
17. Cabana, J., *et al.* Composition-Structure Relationships in the Li-Ion Battery Electrode Material $LiNi_{0.5}Mn_{1.5}O_4$. *Chem. Mater.* **24**, 2952-2964 (2012).
18. Liu, J., Kunz M., Chen, K., Tamura, N., & Richardson, T.J. Visualization of Charge Distribution in a Lithium Battery Electrode. *J. Phys. Chem. Lett.* **1**, 2120-2123 (2010).
19. Meirer, F., Cabana, J., Liu, Y., Mehta, A., Andrews, J.C., & Pianetta, P. Three-dimensional Imaging of Chemical Phase Transformation at the Nanoscale with Full-Field Transmission X-ray Microscopy. *J. Synchrotron Rad.* **18**, 773-781 (2011).
20. Liu, X., *et al.* Phase Transformation and Lithiation Effect on Electronic Structure of Li_xFePO_4: An In-Depth Study by Soft X-ray and Simulations. *J. Am. Chem. Soc.* **134**, 13708-13715 (2012).
21. Sokaras, D., *et al.* A High Resolution and Solid Angle X-ray Raman Spectroscopy End-Station at the Stanford Synchrotron Radiation Lightsource. *Rev. Sci. Instrum.* **83**, 043112 (2012).
22. Chan, M.K.Y., *et al.* Structure of Lithium Peroxide. *J. Phys. Chem. Lett.* **2**, 2483-2486 (2011).

